Journal of Cereal Science 83 (2018) 74–82

Contents lists available at ScienceDirect

Journal of Cereal Science

journal homepage: www.elsevier.com/locate/jcs

Does Fe accumulation in durum wheat seeds benefit from improved whole-plant sulfur nutrition?

Stefania Astolfi[a,*], Youry Pii[b], Roberto Terzano[c], Tanja Mimmo[b], Silvia Celletti[a,b], Ignazio Allegretta[c], Domenico Lafiandra[a], Stefano Cesco[b]

[a] DAFNE, Università Degli Studi Della Tuscia, Viterbo, Italy
[b] Faculty of Science and Technology, Free University of Bozen-Bolzano, I-39100, Bolzano, Italy
[c] Di.S.S.P.A, Università Degli Studi di Bari, Bari, Italy

ARTICLE INFO

Keywords:
Biofortification
Iron
Sulfur
Triticum durum
μ – XRF

ABSTRACT

Sulfur and iron balanced supply is of paramount importance for plants, since Fe homoeostasis in plants has been shown to be strongly dependent on sulfate availability; *vice versa* the adaptation to Fe deficiency requires the adjustment of S uptake and assimilation rate. Interestingly, it has been demonstrated that providing S above adequate concentrations may enhance Fe use efficiency in wheat and this effect seems to be especially advantageous for plants grown under severe Fe shortage. Therefore, the investigation of sulfate effect on Fe uptake and allocation in crop could be of great significance.

Aim of this study was to clarify in wheat at both leaf and seed level whether and to what extent the changes in S and Fe supply affect concentration and distribution of sulfate and also how different availability of S changes the mineral concentration and distribution in wheat adequately or poorly fed with Fe.

Obtained results showed how plants recovered from Fe deficiency stress by means of a tuned S fertilization, without additional input of Fe fertilizers. Also, with decreasing Fe availability the Zn concentration of grains significantly increased, suggesting that a balanced crop Fe nutrition could allow a successful biofortification of wheat grains with Zn.

1. Introduction

Iron (Fe) is one of the most critical nutrients, being not only one of the main causes of yield limitation of crops in the World but also one of the most widespread human nutritional disorders affecting over 30% of the World's population (Hind and Guerinot, 2012). Cereals are the primary food source for humans, particularly in developing countries; thus, the nutritional level of the grain (as well as the nutritional state of plants) is of central importance to human health (Grusak and Dellapenna, 1999). Both plants and humans need an adequate supply of minerals for their nutrition; in this regard, the acquisition of Fe from soil can be often problematic for plants.

Iron is sparingly soluble under aerobic conditions, especially in high pH and calcareous soils, representing a serious problem for more that 30% of the World's cultivated soils (Guerinot and Yi, 1994). To cope with this nutritional disorder and to favour the micronutrient acquisition, higher plants have developed specific strategies (Marschner et al., 1986). In particular, graminaceous species cope with Fe deficiency stress by enhancing the exudation of phytosiderophores (PS) into the rhizosphere. These non-proteinogenic amino acids belonging to the mugineic acid family, form stable complexes with Fe^{3+} and are taken up by roots as intact Fe^{3+}–PS complexes *via* the Yellow Stripe 1 (YS1) transporter (Murata et al., 2006). Iron metabolism in plants is closely linked to sulfur (S) since the sulfur-containing amino acid methionine (Met) is the sole precursor of the mugineic acid family of PS (Mori and Nishizawa, 1987). In fact, it has been clearly demonstrated that plant capability to take up and accumulate Fe is strongly dependent on S availability in the growth medium in cereal plants (Bouranis et al., 2003; Astolfi et al., 2006; Zuchi et al., 2012). On the other hand, the modulation of S uptake and assimilation rate play a significant role in the plant adaptation to the changes of Fe availability (Ciaffi et al., 2013; Celletti et al., 2016a). For instance, it has been shown that a super-optimal S feeding (2.4 mM vs 1.2 mM which is considered as optimal) favours an accumulation of Fe in shoots of durum wheat (Zuchi et al., 2012). Recently, it has been observed a positive correlation between changes in S accumulation and plant capability to release PS (and correspondingly to accumulate Fe), indicating that a super-optimal S fertilization of plants can increase the Fe use efficiency of roots. Since

* Corresponding author. Universita degli Studi della Tuscia – DAFNE, Via San Camillo de Lellis, 01100, Viterbo, Italy.
E-mail address: sastolfi@unitus.it (S. Astolfi).

https://doi.org/10.1016/j.jcs.2018.07.010
Received 19 June 2018; Received in revised form 19 July 2018; Accepted 21 July 2018
Available online 23 July 2018
0733-5210/

this phenomenon is specifically observed in wheat plants, this plant species could represent a potentially useful model system to study S/Fe interactions (Celletti et al., 2016b). These findings open a significant outlook on exploring potential and sustainable use of S nutrition in improving Fe distribution within the plant and its accumulation into grains of durum wheat. The Fe-S interplay might be exploited from both a scientific and an applicative point of view identifying both the response mechanisms associated with multiple deficiency and developing agronomic practices aimed at increasing Fe acquisition from soil (i.e. more sustainable agriculture) and at obtaining biofortified agricultural products (Welch and Graham, 2004). In fact, one of the most important challenges to be met in the next future is also to increase the nutritional value of the agricultural products, like the content of Fe. However, in this respect, the evidence concerning the possible contribution of an over availability of S in the accumulation of Fe at the seed level of cereals is still missing.

Starting from these premises, this study focused on the potential effects of S application rates and concentrations on plant capability to accumulate Fe in grains especially in Fe-deficient conditions. To this aim, durum wheat plants were grown on sand/perlite mixture under two different S and Fe supplies throughout the growing season. At harvest, plants samples and seeds were collected and analysed for their nutrients content by inductively coupled plasma-optical emission spectroscopy (ICP-OES). The distribution of the nutrients, in particular of S and Fe, in whole seeds and seed sections was assessed by micro-focused X-ray fluorescence (μ−XRF) imaging. Recently Lemmens et al. (2018) showed the high relevance of μ−XRF imaging data in studying element distribution in wheat grains. Data of plant and seed analysis are discussed in relation to the S and Fe availability levels in the growth medium.

2. Materials and methods

2.1. Growth conditions

Seeds of durum wheat (*Triticum durum* L. cv. Svevo) were germinated on moistened paper in the dark at 20 °C for 4 d. Seedlings were then transferred in 20 cm diameter plastic pots (three seedlings in each pot) filled with 3 L of 50% (v/v) sand/perlite mixture as substrate and were grown in the greenhouse (a low-technology model in which the active environmental control was limited to a natural ventilation system through wall and roof windows and the photoperiod was provided by natural sunlight). Plants were watered with 1 L pot^{-1} of nutrient solution (1 L pot^{-1}) (NS) (Zhang et al., 1991) was applied from above every other day (three times per week, Monday, Wednesday and Friday) and with 1 L pot^{-1} of demineralised water on the other days (three times per week, Tuesday, Thursday and Saturday). Pots were allowed to drain freely to prevent any accumulation of nutrients in pots.

The experiment examined the effect of two target sulfate concentrations (*i.e.*1.2 and 2.4 mM) on Fe accumulation in durum wheat plants and grains. Sulfate concentrations in the NS were selected and applied according to our previous report (Zuchi et al., 2012; Celletti et al., 2016b). The highest concentration was considered as extra sulfate supply condition and labelled with E, whereas the lowest concentration was considered as sufficient condition and labelled with C. Furthermore, NS was supplemented with two different concentrations of Fe (III)-EDTA (10 and 80 μM, deficiency and sufficiency condition, respectively).

Thus, the treatments were consisted on two factors, sulfate and iron, and two levels of each factor were taken, determining four different conditions, listed as follows: C = control (1.2 mM sulfate and 80 μM Fe^{III}-EDTA), F = Fe deficiency (1.2 mM sulfate and 10 μM Fe^{III}-EDTA), E = excess S supply (2.4 mM sulfate and 80 μM Fe^{III}-EDTA) and EF = excess S supply and Fe deficiency (2.4 mM sulfate and 10 μM Fe^{III}-EDTA).

Nutrient solution, containing both sulfate and Fe^{III}-EDTA, was supplied to the plants until maturity (about 56 days post anthesis); after this point the plants were left without water to allow them to senesce prior to harvest at 170 days after sowing. At harvest, whole plants were collected by cutting them at the stem base, separated into shoots (stems + leaves) and ears. To estimate grain yield, ears were hand-harvested and counted (number of ears per plant) and grains were weighed (g per plant) to obtain mean grain yield.

The experiment was arranged as a completely random design with three replications (pots) and the pots were randomly moved daily to minimize position effects.

2.2. Chlorophyll content

The chlorophyll content per unit area was estimated in attached leaves by a portable apparatus (SPAD-meter, Minolta Co., Osaka, Japan) using the first fully expanded leaf from the top of the plant. Recordings were conducted approximately every week during the whole experimental period.

2.3. Analysis of micro- and macronutrient concentrations

Shoot tissues and grains were dried to a constant weight at 80 °C, weighed and acid digested with concentrated ultrapure HNO_3 (65% v/v, Carlo Erba, Milano, Italy), using a Single Reaction Chamber (SRC) microwave digestion system (UltraWAVE, Milestone, Shelton, CT, USA). The elements concentration was subsequently analyzed by ICP-OES (Spectro Arcos, Spectro, Germany). Elements quantifications were carried out using certified multi-element standards (CPI International, https://cpiinternational.com). Tomato leaves (SRM 1573a) and spinach leaves (SRM 1547) have been used as external certified reference material.

To determine total S concentration, shoot and root tissues and grains were homogenized and one g of each sample was dried at 80 °C and then ashed in a muffle furnace at 500 °C. The ashes were dissolved in 10 mL of 3 N HCl and filtered through Whatman No. 42 paper. In contact with $BaCl_2$, a $BaSO_4$ precipitate is formed which is determined turbidimetrically (Bardsley and Lancaster, 1960).

2.4. Micro-focused X-ray fluorescence (μ−XRF) imaging

Micro X-ray fluorescence maps were collected by a laboratory benchtop μ-XRF spectrometer (M4 Tornado, Bruker Nano GmbH, Berlin, Germany). This instrument is equipped with a micro-focus Rh X-ray source (50 kV, 600 μA), a polycapillary X-ray optics with a spotsize of 25 μm and two XFlash™ energy dispersive silicon drift detectors with 30 mm^2 sensitive area and an energy resolution of 140 eV @ Mn K_α. The two detectors, placed at opposite sites compared to the X-ray optics, allow to reduce shadowing effects in the elemental maps. Wheat grains were impregnated in epoxy resin and sectioned both longitudinally (along the crease tissue) and transversely (at the middle of the seed). The cut seeds where then glued on glass slides with an epoxy resin and trimmed to 200 μm thickness. All the analyses were performed under reduced pressure (20 mbar) by acquiring one spectrum every 20 μm step, with an acquisition time of 20 ms per step. In order to increase the signal-to-noise ratio, each sample was scanned 30 times and the spectra averaged. XRF hyperspectral data and images were processed with the ESPRIT™ built-in software from the M4 Tornado. All the maps were collected with the same analytical conditions and the same scale was used for the same element in all the maps. Therefore the elemental maps can be compared for the same element and brighter colors mean a higher concentration of the element. Three sections (both longitudinal and transverse) from three different seeds were prepared and analysed for each treatment. Results were similar within the same treatment, therefore only the images from one section for each treatment are shown as representative of the treatment. Correlation maps were obtained by using the software Datamuncher (Alfeld and Janssens, 2015),

which was used to obtain both the sum spectrum and the maximum pixel spectrum of each XRF database. Then, the fitting of the sum spectrum was performed with the software PyMCA (Solè et al., 2007) and the maximum pixel spectrum was checked in order to consider also those elements which were detected only in few parts of the section. Fitting parameters were imported in Datamuncher in order to perform the fitting of each pixel of the database and then a new database containing the net area related to each fluorescence line per pixel was produced. Since the analysed samples were prepared and acquired in the same conditions, the new produced databases were merged. Then, scatterplots were obtained plotting the net area of a fluorescence line of an element against another fluorescence line for each pixel. When correlations were found, they were marked with different colours and the related sample portions were shown.

2.5. Statistical analysis

Each reported value represents the mean ± SD of measurements carried out in triplicate and obtained from four independent experiments. Statistical analyses of data were carried out by ANOVA with the GraphPad InStat Program (version 3.06). Significant differences were established by posthoc comparisons (HSD test of Tukey) at $P < 0.05$. Pairwise comparisons have been carried out by Student's t-test. Multivariate analyses (Principal Component Analysis-PCA) were carried out by using PAST 3.14 software for Mac OSX. The validity of the PCA models were assessed by the cross-validation approach previously described (Pii et al., 2015a).

3. Results

3.1. Effect of nutrients supply on growth and yield of wheat plants

Visual observations and SPAD readings (Fig. 1A) indicated that the highest chlorophyll levels were observed in plants subjected to E treatment (Fe-sufficient plants supplied with 2.4 mM sulfate), followed by C plants (Fe-sufficient plants supplied with 1.2 mM sulfate). The chlorophyll content in Fe-deficient plants (both F and EF) reflected chlorosis induction typical of Fe deficiency (Fig. 1A). In general, plants submitted to high S concentrations (E treatment), showed higher SPAD values compared to control plants, irrespective of Fe supply.

In Fig. 1B the yield parameters are separated into the two main components: number of ears and mean weight of grains per plant. The highest ear number per plant (7.8) as well as the highest yield (20.93 g plant^{-1}), expressed as grain weight per plant, were obtained with C treatment. The lack of Fe in the nutrient solution (F plants) induced a significant reduction (about 30%) of the weight of grain produced by wheat plants as compared to C plants (Fig. 1B). On the other hand, the EF plants displayed a similar yield as C plants, and higher than F plants (26%), suggesting that somehow extra sulfate supply at least partially reduced yield losses due to Fe deficiency.

3.2. Nutrient allocation in seed and leaves

A significant S increase (+30% vs the control) in plant shoots supplied with high S supply (E condition) was detected, whereas sole Fe deficiency (F condition) resulted in a large and significant decrease in total S content of the shoots (−20% vs the control) (Fig. 1C). On the other hand, Fe-deficient plants supplied with extra S (EF condition) revealed approximately the same tissue-S content as observed in the control (C condition); however, these concentrations resulted lower (−25%) than their respective control (E condition) (Fig. 1C). Total S content in grains did not show a significant response to both sole extra S (E condition) and sole Fe deficiency (F condition), whereas we observed a decrease of about 25%, although not significant, with respect to control when plants were exposed to Fe deficiency in combination with extra S (EF condition) (Fig. 1C).

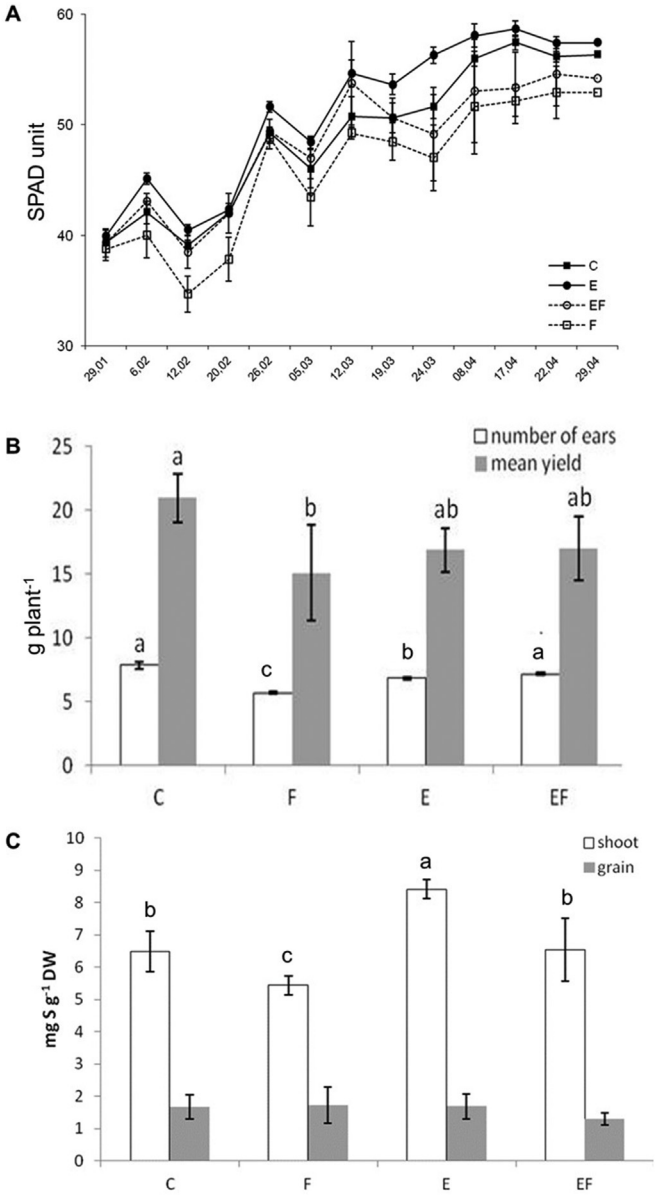

Fig. 1. Chlorophyll levels measured using a SPAD meter in leaves of wheat plants (A), mean number of ears per plant (white bars) and mean grain yield (g per plant) (grey bars) (B) and total S content in shoots (white bars) and grains (grey bars) of wheat plants (C). Plants were grown being exposed to different four treatments: C = control (1.2 mM sulfate and 80 mM Fe^{III}-EDTA), F = Fe deficiency (1.2 mM sulfate and 10 mM Fe^{III}-EDTA), E = excess S supply (2.4 mM sulfate and 80 mM Fe^{III}-EDTA) and EF = excess S supply and Fe deficiency (2.4 mM sulfate and 10 mM Fe^{III}-EDTA). Data are means ± SD of four independent replications run in triplicate. The statistical significance was tested by means of ANOVA with Tukey post-test. Different letters indicate statistically different values ($P < 0.05$).

Besides S, the total ionomic profile of both shoots and seeds of wheat plants (Figs. 2 and 3, Supplementary Table 1) was assessed to reveal whether the nutritional conditions imposed to wheat plants influenced both the uptake and the allocation of mineral elements in the aboveground organs (*i.e.* shoots and seeds). The Principal Component Analysis (PCA) carried out on the shoot ionome produced a three-components model accounting for a total variance of about 99.88%, with PC1 86,753%; PC2 6409%; PC3 4316% (Fig. 2). Since combining either PC1-PC2 or PC1-PC3 we obtained a coverage of the total variance higher than 90%, we chose to use the PC1-PC3 combination because we could achieve a better separation of samples according with the

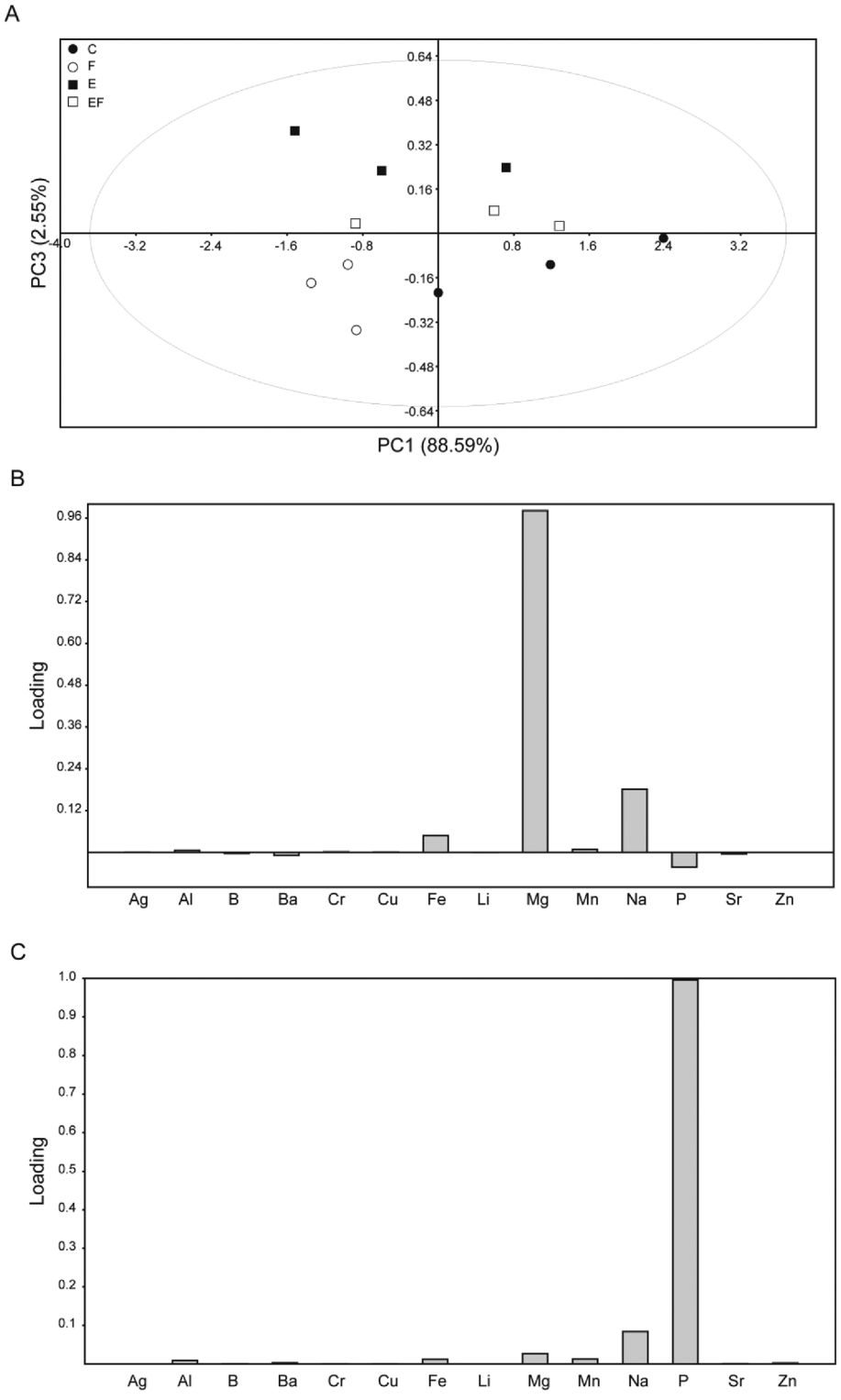

Fig. 2. Principal components analysis (PCA) of the shoot ionome of wheat plants. Plants were grown being exposed to different four treatments: C = control (1.2 mM sulfate and 80 mM Fe^{III}-EDTA), F = Fe deficiency (1.2 mM sulfate and 10 mM Fe^{III}-EDTA), E = excess S supply (2.4 mM sulfate and 80 mM Fe^{III}-EDTA) and EF = excess S supply and Fe deficiency (2.4 mM sulfate and 10 mM Fe^{III}-EDTA). (A) Scatterplot representing the modification of the shoot ionome as a function of the nutritional regime. (B) Loading plot representing the contribution of each variable included in the PCA model on the samples distribution along the PC1. (C) Loading plot representing the contribution of each variable included in the PCA model on the samples distribution along the PC3.

treatments imposed. The same also applied for the ionomic data of seeds. Indeed, also in this case a three components model was obtained, featuring PC1 88,585%; PC2 8746%; PC3 2548% (Fig. 3). The scatterplot obtained combining the PC1 and PC3 describes 91.13% of the total variance and, along PC3, it shows the separation of the samples according to the sulfate concentration in the nutrient solution (*i.e.* 1.2 mM vs. 2.4 mM) (Fig. 2A). As shown by the loading plot, the highest positive contribution to the separation along PC3 (2.55%) is given by magnesium (Mg, $p < 0.0001$), that resulted highly accumulated in the leaves of plants grown in the presence of higher concentration of sulfate, regardless the Fe nutritional status (Fig. 2B). As already observed (Zuchi et al., 2012; Celletti et al., 2016b), Fe had a higher concentration in shoots of plants grown in nutrient solution containing 2.4 mM sulfate with respect to control plants (Figs. 2B and 4A). In particular, when comparing Fe deficient plants we found that there was a significant increase (+35%) in shoot Fe concentration of E plants with respect to EF ones (Fig. 4A). Furthermore, it is important to note that the reduction of Fe accumulation in shoots induced by Fe deficiency condition

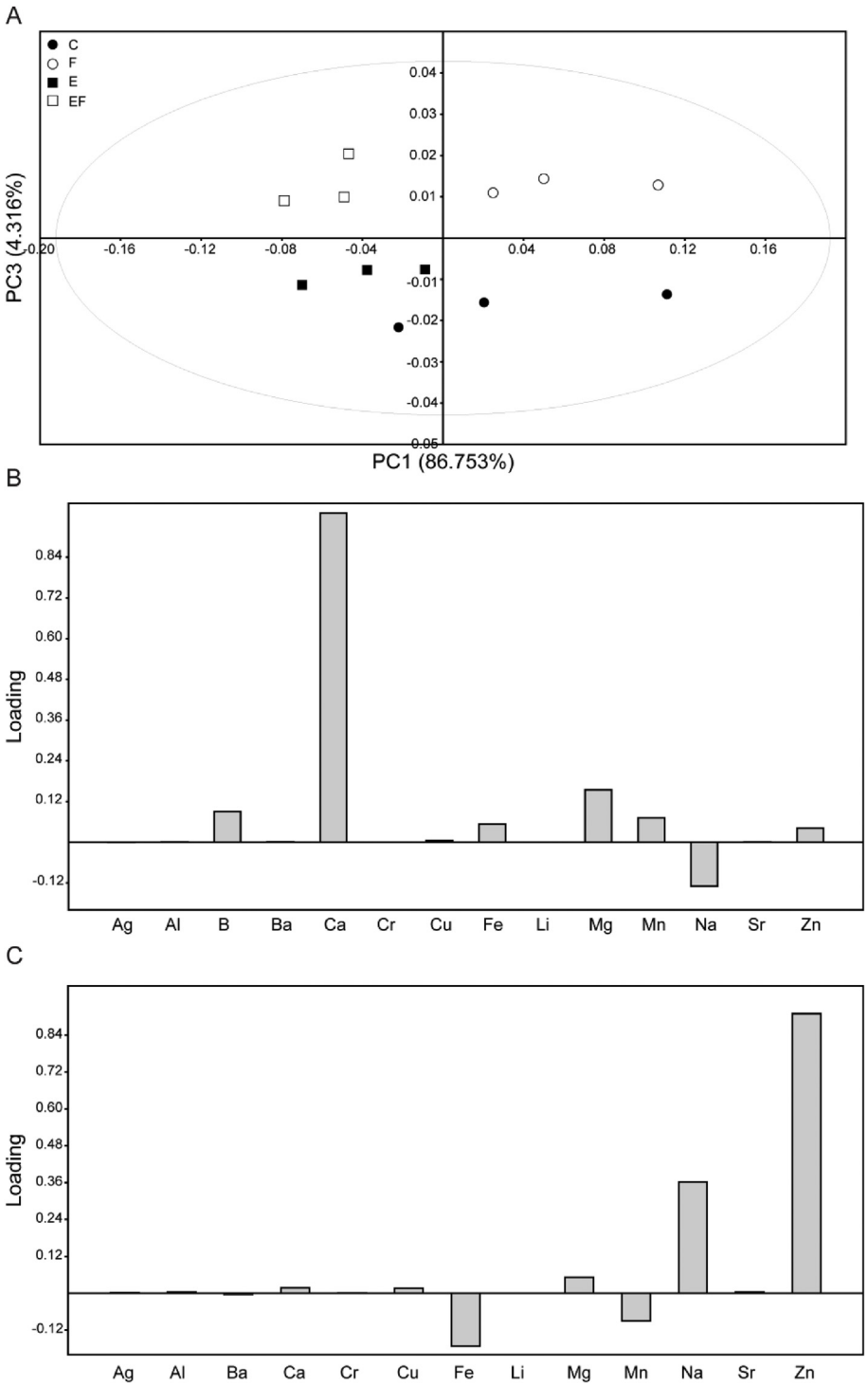

Fig. 3. Principal components analysis (PCA) of the seed ionome of wheat plants. Plants were grown being exposed to different four treatments: C = control (1.2 mM sulfate and 80 mM Fe^{III}-EDTA), F = Fe deficiency (1.2 mM sulfate and 10 mM Fe^{III}-EDTA), E = excess S supply (2.4 mM sulfate and 80 mM Fe^{III}-EDTA) and EF = excess S supply and Fe deficiency (2.4 mM sulfate and 10 mM Fe^{III}-EDTA). (A) Scatterplot representing the modification of the seed ionome as a function of the nutritional regime. (B) Loading plot representing the contribution of each variable included in the PCA model on the samples distribution along the PC1. (C) Loading plot representing the contribution of each variable included in the PCA model on the samples distribution along the PC3.

was potentially alleviated with increasing S application (−60% in F condition and only −40% in EF condition, with respect to their relative Fe-sufficient control, C and E, respectively) (Fig. 4A). Considering the PC1 (88.59%), samples grown in the presence of the lower sulfate concentration showed a clusterization according to the Fe nutritional status; in fact the distribution along the positive direction of the axis is mainly driven by the concentration of Fe; also the concentration of phosphorus (P) is higher in Fe sufficient plants (Fig. 2C and Supplementary Table 2).

The multivariate analysis carried out on the ionomic profile of seeds generated a model composed of three principal components, accounting for approximately 97.48% of the total variance. The scatterplot obtained combining the PC1 (86.75%) and the PC3 (4.32%) showed the separation of samples in four distinct clusters (Fig. 3A). Interestingly, along the PC1, samples clustered according to the S provision (Fig. 3A), pointing out at elements like calcium (Ca), Mg, manganese (Mn) and zinc (Zn) as the stronger drivers for the positive direction of the axis (Fig. 3B). Indeed, the accumulation of Ca resulted statistically higher ($p < 0.001$) in those plants that were provided with a lower concentration of S in the nutrient solution, regardless the Fe nutrition. In addition, the concentration of Fe was significantly higher ($p = 0.0048$) in the seeds produced by plants grown in the presence of a lower concentration of sulfate (*i.e.* C and F plants, Fig. 4A); these observations might suggest that the mechanisms involved in the allocation of Fe in

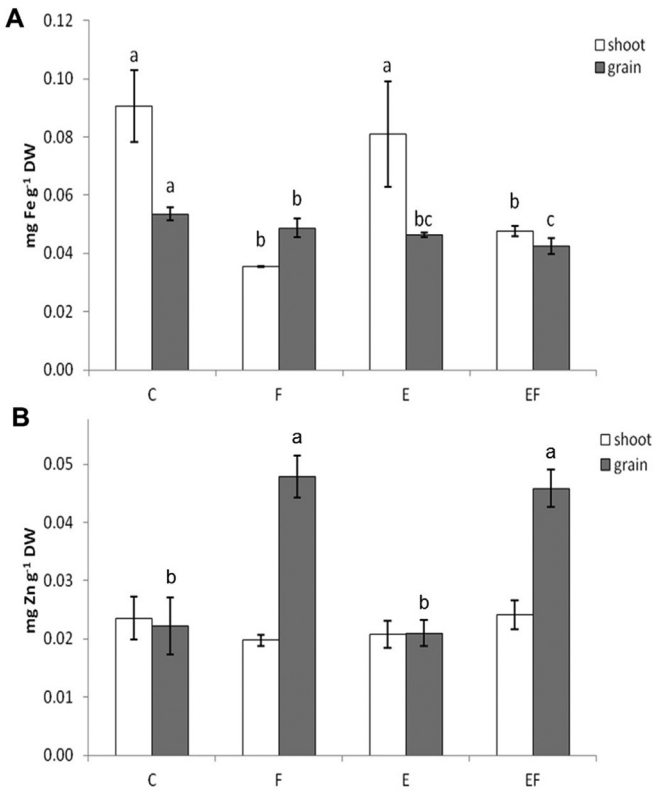

Fig. 4. Iron (A) and zinc (B) concentration in shoots (white bars) and grains (grey bars) of wheat plants. Plants were grown being exposed to different four treatments: C = control (1.2 mM sulfate and 80 mM Fe^{III}-EDTA), F = Fe deficiency (1.2 mM sulfate and 10 mM Fe^{III}-EDTA), E = excess S supply (2.4 mM sulfate and 80 mM Fe^{III}-EDTA) and EF = excess S supply and Fe deficiency (2.4 mM sulfate and 10 mM Fe^{III}-EDTA). Data are means ± SD of four independent replications run in triplicate. The statistical significance was tested by means of ANOVA with Tukey post-test. Different letters indicate statistically different values ($P < 0.05$).

seeds might be different from those controlling the root uptake and the allocation in the leaves. On the other hand, we found that at lower Fe concentration (F and EF conditions) wheat plants accumulated in grains higher Zn concentration, which reached values two-fold higher than the respective Fe-sufficient control (C and E conditions) (Fig. 4B). The third component showed a net separation of the samples according to the Fe nutrition (Fig. 3A) and, in this case, the distribution was determined by Zn ($p < 0.001$) and Cu ($p < 0.05$), in the positive direction, and by Fe and Mn in the negative direction (Fig. 3C and Supplementary Table 3).

3.3. Element distributions in seeds

Elemental distribution maps were collected on thin sections (200 μm) cut both longitudinally and transversely from the seeds. However, as also reported by Ramos et al. (2016), cutting the seeds longitudinally along the crease tissue may cause an uneven distribution of the seed components, which may result in sections that cannot be directly compared. Differently, transverse sections cut at the middle of the seed are more directly comparable, containing substantially the same components for all samples, as also evidenced by Ajiboye et al. (2015). Therefore, only data obtained from transverse sections are presented. Representative elemental distribution maps for some major elements (K, P, S, Ca) and micronutrients (Zn, Fe, Mn, Cu) are reported in Fig. 5. As it can be seen in Fig. 5B, in all seeds, K appears distributed mainly in the pericarp. Except for F sample, K concentration is almost homogenous throughout all the pericarp, with only a reduction in the creased tissues. Phosphorus (Fig. 5C) appears also mostly concentrated

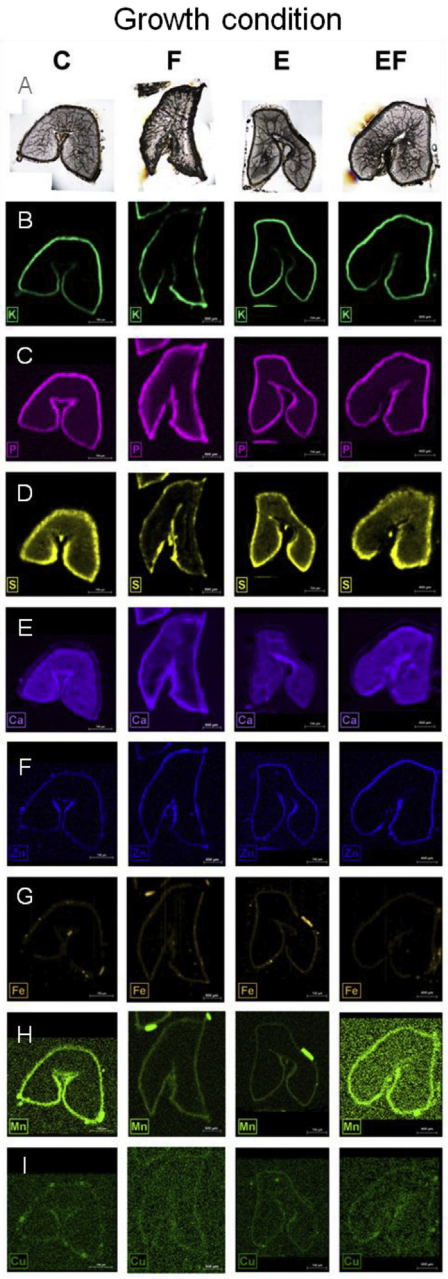

Fig. 5. Representative μ-XRF distribution maps for some major elements (K, P, S, Ca, into B, C, D and E boxes, respectively) and micronutrients (Zn, Fe, Mn, Cu, into F, G, H and I boxes, respectively) for wheat seed thin sections. Seeds were obtained from wheat plants grown being exposed to different four treatments: C = control (1.2 mM sulfate and 80 mM Fe^{III}-EDTA), F = Fe deficiency (1.2 mM sulfate and 10 mM Fe^{III}-EDTA), E = excess S supply (2.4 mM sulfate and 80 mM Fe^{III}-EDTA) and EF = excess S supply and Fe deficiency (2.4 mM sulfate and 10 mM Fe^{III}-EDTA). Brighter colors correspond to higher element concentrations. Only maps for the same element are directly comparable in terms of concentrations. Optical transmission microscopy images of the sectioned seeds are also reported (box A). (For interpretation of the references to colour in this figure legend, the reader is referred to the Web version of this article.)

in the pericarp but in F sample it is also present in the aleurone layer. Differently from K, P concentration is almost identical throughout all the pericarp. Sulfur (Fig. 5D) appears concentrated both in the pericarp and the aleurone but it is also present in the endosperm, with the only exception of sample F where the concentration in the endosperm and the aleurone is much lower than the pericarp. A high S concentration is

also observed in the vascular bundle. In all samples, Ca is distributed in the pericarp while, except for sample F, no Ca is present in the aleurone layer (Fig. 5E). Calcium is also visible in the endosperm. The higher concentration around the starch grains (reticulate pattern) is probably due to the glass support behind the thin section. In all samples, a higher Ca concentration is visible in the crease tissues. In all samples, Zn appears distributed in the pericarp, with higher concentrations in the areas surrounding the crease tissues (Fig. 5F). Iron also appears mostly distributed in the pericarp in all samples (Fig. 5G). Some hotspots are probably due to seed coat residues. However, Fe concentration in the grain is close to the detection limit of the instrument and therefore Fe signal is very weak, as also reported by Ramos et al. (2016). Similarly to Fe, Mn is mostly concentrated in the pericarp with concentrations close to the detection limit (Fig. 5H). The presence of Mn is also visible in the crease tissue, as also imaged at higher resolution by Ajiboye et al. (2015). Copper distribution is very noisy and does not allow making particular considerations (Fig. 5I). From these data the difference between sample F and all the other seeds is evident, especially for Ca, P and S distributions. Micronutrients do not show particular differences among the samples.

A better discrimination among the four types of samples can be visualized by correlation maps. Correlation maps show with different colors (red, green, blue and purple) the pixels in the μ-XRF images characterised by specific selected ratios between a pair of elements. These ratios are selected from binary correlation graphs (scatterplots) reporting the XRF signal intensities of the elements for each pixel of the image. Correlation maps and binary correlation graphs are presented in Fig. 6. In Fig. 6A, correlation maps of K vs Ca are presented. These maps, besides confirming the large difference of sample F, where the K to Ca ratio in the pericarp is much lower than in the other samples, highlight some differences also among the other samples. In particular, while the K vs Ca ratio is similar for samples E and EF, sample C shows three distinct domains. A first domain of higher K/Ca values is distributed in the dorsal pericarp region (blue), an intermediate one in the ventral pericarp region (purple) and a lower K/Ca in the crease region (green). Also the P vs K ratio shows some differences between sample C and E or EF (Fig. 6B). In general, the P/K values are higher in the pericarp of C sample compared to E and EF, while the ratio in the crease pericarp is similar. In sample F the P/K values are high throughout all the pericarp, without differences of distribution. The distributions of S vs P intensities (Fig. 6C) clearly discriminate the three main components of the seed in samples E, EF and C: the pericarp (red), the aleurone (blue) and the endosperm (green). This ratio is very similar for all these three samples while it is completely different for F sample where the separation of the three components is not evident, with a prevalence of lower S/P values. For the S/Fe ratio (Fig. 6D), a similar distribution is visible for all the samples as far as the pericarp and the aleurone layers are concerned. However, the S/Fe ratio in the endosperm is completely different in the F sample compared to the other three sections, being the S/Fe ratio in the endosperm of the F sample similar to that in the pericarp (red) while the other samples show a much higher S/Fe ratio.

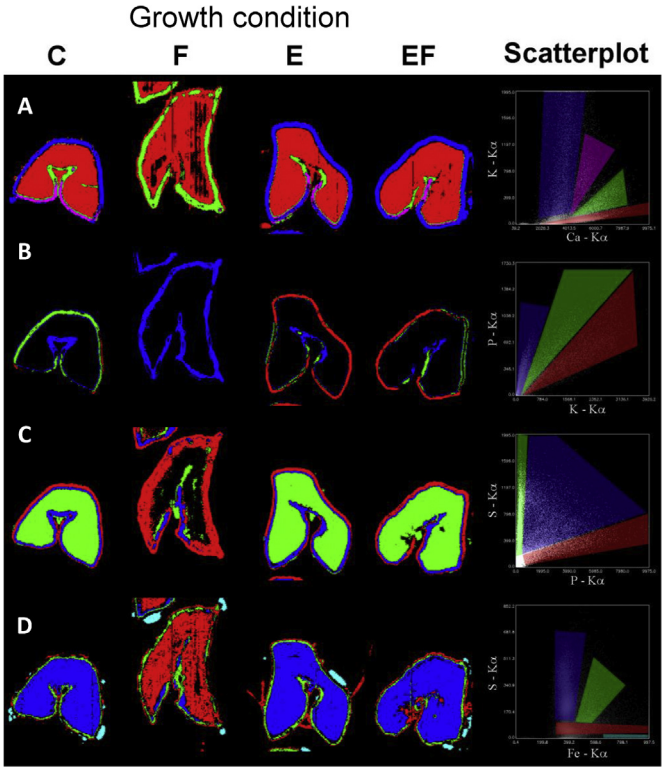

Fig. 6. Representative μ-XRF correlation maps of K/Ca (A), P/K (B), S/P (C) and S/Fe (D). Scatterplots of the elemental XRF signal intensities are also reported for each element pair.

4. Discussion

The present study aimed at investigating the potential and sustainable use of S nutrition in improving Fe accumulation in grains of durum wheat. For this purpose we set up an experiment in which durum wheat plants were supplied with two different S levels, sufficient (1.2 mM) and high (2.5 mM) and two different Fe levels, sufficient (80 μM Fe-EDTA) and limited (10 μM Fe-EDTA). Thereby, we hypothesized that the accumulation of Fe into grains was affected by S fertilization in the same extent as the shoot Fe accumulation (Zuchi et al., 2012; Celletti et al., 2016b).

In general, leaf chlorophyll content is strongly influenced by both S and Fe availability (Marschner, 2012). Accordingly, the highest and the lowest SPAD values were induced by the treatment E and F, respectively (Fig. 1A). The lowest chlorophyll concentration induced by the F condition was accompanied by strong limitations in yield parameters, in terms of both number of ears and mean weight of grains per plant (Fig. 1B). Interestingly, differences between the two S supply treatments (C and E) were detected in terms of number of ears, but not of mean yield, as well as between the F and EF conditions (Fig. 1B). However, whereas the mean yield of F plants was clearly lower than that of C plants, exposure to EF condition resulted in yield level similar to that of control plants (Fig. 2). Both SPAD values (Fig. 1A) and yield parameters (Fig. 1B) were positively affected by extra sulfate supply that, therefore, seems to allow a partial recovery of Fe deficiency symptoms.

There are several studies demonstrating that the rebalance of sulfate uptake and assimilation rates is very active in grasses exposed to Fe deficiency stress (Astolfi et al., 2006; Ciaffi et al., 2013; Celletti et al., 2016a) leading to an increased S concentration in plant tissues with decreasing Fe concentration (Celletti et al., 2016a). This response was ascribed to the increased demand of reduced S for methionine and, consequently, PS synthesis induced by the Fe deprivation. In contrast, the present study indicates that in long-term experimental period Fe shortage is not responsible for the increased S accumulation, as it occurs in short-term experiments. In particular, the shoot S accumulation of the Fe-stressed (F) plants was 20% lower than that of the C ones and the situation was even worse when Fe deficiency was imposed on extra S supply (EF condition), with a negative effect of on both shoot and grain S concentration (about 25% lower than control) (Fig. 1C).

On the other hand, as already reported in previous papers (Zuchi et al., 2012; Celletti et al., 2016b), the superoptimal S supply helped the plants to accumulate higher Fe amounts in shoots (Figs. 2B and 4A) and more importantly, to mitigate the effect of Fe deficiency. In fact, in F plants Fe accumulation in shoots resulted 60% lower compared to the control, while in EF plants the accumulation was only 40% lower than in E plants (Fig. 4A). However, high S supply did not increase the Fe

concentrations of grains. Surprisingly, the concentration of Fe was significantly highest ($p = 0.0048$) in the seeds produced by plants grown in the presence of a lower concentration of sulfate (*i.e.* C and F plants), suggesting that the mechanisms controlling the allocation of Fe in seeds might be different from those controlling the root uptake and allocation in the leaves of the micronutrient. Yet, the detailed Fe distribution in grains by μ-XRF images did not confirm the quantitative analysis showing a uniform allocation in the pericarp (Fig. 5G). Nonetheless, we cannot exclude that a differential accumulation of Fe might be present in other grain organs, which are not displayed in our sections. Accordingly, a recent study (Wu et al., 2013) highlighted that nutrients such as Cu, Fe, K, Mg, Mn, P and Zn are mostly accumulated in the scutellum. Results by Lemmens et al. (2018) reported a slightly different element distribution in grains of *Triticum aestivum* L. compared to those reported in our study for *Triticum durum* L., with Fe and Zn mostly concentrated in the aleurone layer and colocalized with P, suggesting the formation of Fe- and Zn-phytate complexes. However, the synchrotron radiation μ-XRF instrument used by the above mentioned authors allowed a much higher resolution (1–3 μm) thus enabling them to better discriminate between the pericarp and aleurone layer whose thickness ranges from about 50 to 100 μm each.

Considering the other elements (especially macronutrients), the distribution was tissue specific and did not vary within the different conditions (Fig. 5) whilst grains from Fe deficient plants revealed completely different element allocation patterns. For instance, P and Ca is mainly concentrated in the aleurone instead of the pericarp, while S is visible only in certain areas of the pericarp and preferentially in the crease area. Usually, S is mainly accumulated in the endosperm reflecting the presence of S-rich storage proteins. Therefore, a reduced S content in the endosperm might negatively affect grain quality and the resulting baking quality parameters (Zhao et al., 1999; Horvat et al., 2012).

Potassium is another important macronutrient, which is crucial for an optimal plant growth and reproduction. Thus, its concentration and distribution in the grains should be tightly regulated. Our results showed that the K allocation was affected only in Fe deficient conditions (Fig. 5B). In general, we observed a decrease in K concentration in the crease area which is thought to be the site of phloem unloading (Thorne, 1985).

The mineral nutrient correlation maps further confirm that the F condition leads to a unique element pattern as compared to the others (Fig. 6). In addition, if plants subjected to Fe deficiency are treated with an excess of S (EF condition) their grain sections totally resemble those obtained from control plants suggesting that a S over-fertilization might overcome abiotic stresses like Fe deficiency (Celletti et al., 2016b). This knowledge in predicting nutrient imbalances and counteracting them is of crucial importance not only considering grain quality but also to ensure an optimal development of the next generation during germination and growth (Bouranis et al., 2018).

It has been widely demonstrated that deficiency conditions of a certain nutrient might cause the imbalance and accumulation of others (Pii et al., 2015a). Furthermore, the nutrient source itself and the physical, chemical and biological soil characteristics, as for instance pH, redox potential and microbial activity (Mimmo et al., 2014; Pii et al., 2015b) affects the availability and consequently plant uptake, translocation and allocation of nutrients.

In fact, in this study we found that the Zn concentration of grains significantly differed in durum wheat grown with adequate or limited Fe availability. Irrespective of the S application level, the Zn concentration in seeds was higher in Fe-limited plants (F and EF) compared with control plants (C and E, respectively) (Fig. 4B). As mentioned earlier for Fe, these differences in Zn concentration could not be confirmed with the qualitative μ-XRF images (Fig. 5F). This result is of great significance for a successful biofortification of wheat grains with Zn by balancing crop Fe nutrition. Zhang et al. (2012) previously reported that with Zn applied as foliar sprays, seed Zn concentration was significantly increased in wheat reaching levels of about 40 mg kg^{-1}, whereas it has been shown here that wheat growth in Fe-limited media resulted in an increase in grain Zn accumulation which reached values even higher than 45 mg kg^{-1}.

In conclusion, our results highlight the importance of understanding the interplay between nutrients. In particular, we showed how a tuned S fertilization might help alleviating Fe deficiency stress without having detrimental effects on the quality of grains. Taken as a whole, this finding could allow the development of a more sustainable agriculture leading to better crop nutrient use efficiency, decrease of chemical inputs and production of healthier food. As regards food quality, this could be a promising approach to potentially increase (biofortification) and preserve important nutrients during food processing (e.g. the effect of S-rich storage proteins on flours' baking quality).

Acknowledgements

The research was carried out in the frame of the MIUR initiative “Department of excellence” (Law 232/2016).

Appendix A. Supplementary data

Supplementary data related to this article can be found at https://doi.org/10.1016/j.jcs.2018.07.010.

The colours in the μ-XRF correlation maps correspond to pixels which have a specific element XRF signal ratio as evidenced by the same colours grouping those pixels in the corresponding scatterplots.

References

Ajiboye, B., Cakmak, I., Paterson, D., de Jonge, M.D., Howard, D.L., Stacey, S.P., Torun, A.A., Aydin, N., McLaughlin, M.J., 2015. X-ray fluorescence microscopy of zinc localization in wheat grains biofortified through foliar zinc applications at different growth stages under field conditions. Plant Soil 392, 357–370.

Alfeld, M., Janssens, K., 2015. Strategies for processing mega-pixel X-ray fluorescence hyperspectral data: a case study on a version of Caravaggio's painting Supper at Emmaus. J. Anal. At. Spectrom 30, 777–789.

Astolfi, S., Cesco, S., Zuchi, S., Neumann, G., Roemheld, V., 2006. Sulfur starvation reduces phytosiderophores release by iron-deficient barley plants. Soil Sci. Plant Nutr. 52, 43–48.

Bardsley, C.E., Lancaster, J.D., 1960. Determination of reserve sulfur and soluble sulfates in Soils[1]. Soil Sci. Soc. Am. J. 24, 265.

Bouranis, D.L., Chorianopoulou, S.N., Protonotarios, V.E., Siyiannis, V.F., Hopkins, L., Hawkesford, M.J., 2003. Leaf responses of young iron-inefficient maize plants to sulfur deprivation. J. Plant Nutr. 26, 1189–1202.

Bouranis, D., Chorianopoulou, S., Margetis, M., Saridis, G., Sigalas, P., 2018. Effect of elemental sulfur as fertilizer ingredient on the mobilization of iron from the iron pools of a calcareous soil cultivated with durum wheat and the Crop's iron and sulfur nutrition. Agriculture 8, 20.

Celletti, S., Pii, Y., Mimmo, T., Cesco, S., Astolfi, S., 2016a. The characterization of the adaptive responses of durum wheat to different Fe availability highlights an optimum Fe requirement threshold. Plant Physiol. Biochem. 109, 300–307.

Celletti, S., Paolacci, A.R., Mimmo, T., Pii, Y., Cesco, S., Ciaffi, M., Astolfi, S., 2016b. The effect of excess sulfate supply on iron accumulation in three graminaceous plants at the early vegetative phase. Environ. Exp. Bot. 128, 31–38.

Ciaffi, M., Paolacci, A.R., Celletti, S., Catarcione, G., Kopriva, S., Astolfi, S., 2013. Transcriptional and physiological changes in the S assimilation pathway due to single or combined S and Fe deprivation in durum wheat (*Triticum durum* L.) seedlings. J. Exp. Bot. 64, 1663–1675.

Grusak, M.A., Dellapenna, D., 1999. Improving the nutrient composition of plants to enhance human nutrition and health 1. Annu. Rev. Plant Physiol. Plant Mol. Biol. 50, 133–161.

Guerinot, M.L., Yi, Y., 1994. Iron: nutritious, noxious, and not readily available. Plant Physiol. 104, 815–820.

Hindt, M.N., Guerinot, M. Lou, 2012. Getting a sense for signals: regulation of the plant iron deficiency response. Biochim. Biophys. Acta Mol. Cell Res. 1823, 1521–1530.

Horvat, D., Drezner, G., Sudar, R., Magdić, D., Španić, V., 2012. Baking quality parameters of wheat in relation to endosperm storage proteins. Croat. J. Food Sci. Technol. 4, 19–25.

Lemmens, E., De Brier, N., Spiers, K.M., Ryan, C., Garrevoet, J., Falkenberg, G., Goos, P., Smolders, E., Delcour, J.A., 2018. The impact of steeping, germination and hydrothermal processing of wheat (*Triticum aestivum* L.) grains on phytate hydrolysis and the distribution, speciation and bio-accessibility of iron and zinc elements. Food Chem. 264, 367–376.

Marschner, H., Romheld, V., Kissel, M., 1986. Different strategies in higher plants in mobilization and uptake of iron. J. Plant Nutr. 9, 695–713.

Marschner, P., 2012. Mineral Nutrition of Higher Plants, third ed. Academic Press, London.
Mimmo, T., Del Buono, D., Terzano, R., Tomasi, N., Vigani, G., Crecchio, C., Pinton, R., Zocchi, G., Cesco, S., 2014. Rhizospheric organic compounds in the soil-micro-organism-plant system: their role in iron availability. Eur. J. Soil Sci. 65, 629–642.
Mori, S., Nishizawa, N., 1987. Methionine as a Dominant Precursor of Phytosiderophores in Graminaceae Plants, vol. 28. pp. 1081–1092.
Murata, Y., Ma, J.F., Yamaji, N., Ueno, D., Nomoto, K., Iwashita, T., 2006. A specific transporter for iron(III)-phytosiderophore in barley roots. Plant J. 46, 563–572.
Pii, Y., Cesco, S., Mimmo, T., 2015a. Shoot ionome to predict the synergism and antagonism between nutrients as affected by substrate and physiological status. Plant Physiol. Biochem 94, 48–56.
Pii, Y., Mimmo, T., Tomasi, N., Terzano, R., Cesco, S., Crecchio, C., 2015b. Microbial interactions in the rhizosphere: beneficial influences of plant growth-promoting rhizobacteria on nutrient acquisition process. A review. Biol. Fertil. Soils 51, 403–415.
Ramos, I., Pataco, I.M., Mourinho, M.P., Lidon, F., Reboredo, F., Pessoa, M.F., Carvalho, M.L., Santos, J.P., Guerra, M., 2016. Elemental mapping of biofortified wheat grains using micro X-ray fluorescence. Spectrochim. Acta Part B At. Spectrosc 120, 30–36.
Solé, V.A., Papillon, E., Cotte, M., Walter, P., Susini, J., 2007. A multiplatform code for the analysis of energy-dispersive X-ray fluorescence spectra. Spectrochim. Acta Part B at. Spectrosc 62, 63–68.
Thorne, J.H., 1985. Phloem Unloading of C and N assimilates in developing seeds. Annu. Rev. Plant Physiol. 36, 317–343.
Welch, R.M., Graham, R.D., 2004. Breeding for micronutrients in staple food crops from a human nutrition perspective. J. Exp. Bot. 55, 353–364.
Wu, B., Andersch, F., Weschke, W., Weber, H., Becker, J.S., 2013. Diverse accumulation and distribution of nutrient elements in developing wheat grain studied by laser ablation inductively coupled plasma mass spectrometry imaging. Metallomics 5, 1276–1284.
Zhang, F.S., Römheld, V., Marschner, H., 1991. Role of the root apoplasm for iron acquisition by wheat plants. Plant Physiol. 97, 1302–1305.
Zhang, Y.-Q., Sun, Y.-X., Ye, Y.-L., Karim, M.R., Xue, Y.-F., Yan, P., Meng, Q.-F., Cui, Z.-L., Cakmak, I., Zhang, F.-S., Zou, C.-Q., 2012. Zinc biofortification of wheat through fertilizer applications in different locations of China. Field Crop. Res. 125, 1–7.
Zhao, F.J., Hawkesford, M.J., McGrath, S.P., 1999. Sulphur assimilation and effects on yield and quality of wheat. J. Cereal. Sci. https://doi.org/10.1006/jcrs.1998.0241.
Zuchi, S., Cesco, S., Astolfi, S., 2012. High S supply improves Fe accumulation in durum wheat plants grown under Fe limitation. Environ. Exp. Bot. 77, 25–32.